

Characterization of the Aerosol Flow, Sampling, and Deposition in a Nose Only Exposure Chamber

Francesco Lucci¹, Wei Teck Tan², Subash Krishnan², Julia Hoeng¹, Patrick Vanscheeuwijck¹, Rudolph Jaeger³, and Arkadiusz Kuczaj^{1,4}

¹ PMI R&D, Philip Morris Products S.A., Quai Jeanrenaud 5, CH-2000 Neuchâtel, Switzerland

² PMI R&D, Philip Morris International Research Laboratories Pte. Ltd., Science Park II, Singapore

³ CH Technologies (USA) Inc., 778 Carver Avenue, Westwood, NJ 07675, USA

⁴ Multiscale Modelling and Simulation, University of Twente, P.O. Box 217, 7500 AE Enschede, The Netherlands

Introduction and Objectives

For *in vivo* drug delivery or toxicological assessment, a variety of inhalation exposure chambers may be employed. In particular, rodent exposure requires efficient and targeted exposure systems. The Nose Only Exposure Chamber (NOEC) produced by CH Technologies (USA) (Figure 1) meets this need and conveys aerosols to separated breathing ports simultaneously. This feature limits other non-respiratory aerosol absorption paths that may complicate biological response analyses, and it also minimizes the amount of test aerosol that is required for the exposure. Any exposure system introduces a certain variability in the aerosol exposure caused either by the system design and functioning principles and/or limited influence to control behavior of the rodents. In our tailored NOEC system, the aerosol mixture flows vertically downward through an inner plenum, and the aerosol is distributed horizontally through 60 exposure ports. These are staggered at 15° offsets between five adjoining tiers of 12 ports each. Ports are loaded with air tight glass tubes to separately house and position the animals. The aerosol is exhausted through an outer plenum peripheral to the inner plenum. A uniform aerosol delivery between all ports is desired for reliable performance of the exposure studies.

The aim of the present analysis is to investigate aerosol flow characteristics in the NOEC system and estimate any potential size-dependent (> 1 μm) aerosol sampling non-uniformities at the animal port. Generally, such insight should lead to better understanding of the operating conditions during exposure and further optimization of the system. For the investigations, we have employed experimental and computational techniques.

The NOEC



Figure 1: Snapshot of a NOEC produced by CH Technologies (USA) and assembled with measurement equipment (Palas) inside a laboratory enclosure.

The NOEC used in the present study was produced by CH Technologies, USA, for Philip Morris International Research Laboratories Singapore to conduct mouse nose-only exposure. In this system, the aerosol mixture flows through an inner plenum, is distributed through 60 exposure ports, and is vented from an outer plenum. The exposure ports are staggered between five tiers of 12 ports each and are loaded with a closed glass tube that supports the animal.

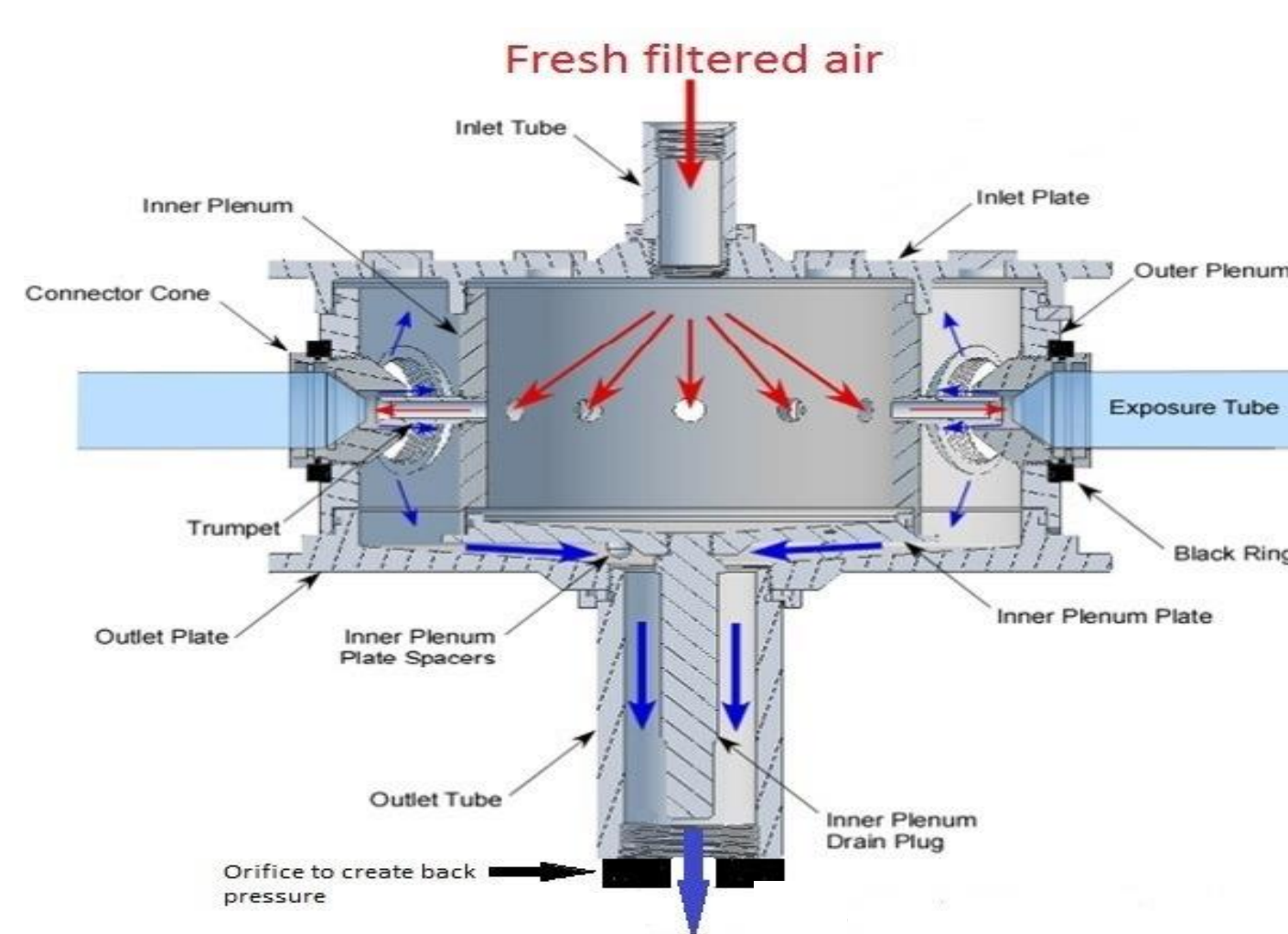


Figure 2: Illustration of flow through the NOEC using a single-tier NOEC. Additional tiers can be added to the NOEC with the flow patterns duplicated in the added components.

An inflow of 33 L/min is supplied to the NOEC, resulting in a minimum flow in each port of about 0.5 L/min, which is consistent with the available guidelines (Wong, Toxicologic Pathology, 35:3–14,2007)

AeroSolved: Platform for Aerosol Numerical Modeling

AeroSolved is a Computational Fluid Dynamics (CFD) code, based on the OpenFOAM software package, for detailed simulation of aerosol dynamics. It is under continuous development to improve its performance and extend its capabilities. In July 2017, it was released to the public domain under the free open source GPLv3 license.

$$\partial_t \rho + \partial_j(\rho u_j) = -\partial_j[(1-\gamma)f_i]$$

$$\partial_t(\rho u_i) + \partial_j(\rho u_i u_j) = -\partial_j p + \partial_j(\mu \tau_{ij})$$

$$\rho c_p(\partial_t T + u_j \partial_j T) = \partial_j(k \partial_j T) + \partial_j(\mu u_k \tau_{kj}) + \frac{DP}{Dt}$$

$$\partial_t(\rho Y_n) + \partial_j(\rho Y_n u_j) = \partial_j(Y^{-1} \gamma f_j Y_n) + S_{Y_n}$$

$$\partial_t(\rho Z_n) + \partial_j(\rho Z_n u_j) = -\partial_j(Z^{-1} f_j Z_n) + S_{Z_n}$$

$$\partial_t(\rho M_q) + \partial_j(\rho M_q u_j) = -\partial_j(\rho M_q u_{j,q}^d) + \partial_j(\rho D_{qj} M_q) + S_{M_q}$$

$$\sum_{n=1}^N (Y_n + Z_n) = 1 \quad Z = \sum_{q=1}^Q s_q M_q$$

Where: N is number of species, Q is number of diameter stencils, Y_n and Z_n are the gas and liquid mass fractions of species n , u^i is the drift velocity, f is correction due to drift, D is coefficient of Brownian diffusion, and S is source terms accounting for evaporation, nucleation, and coagulation.

www.aerosolved.com



On GitHub :

[pmpsa-cfd/aerosolved](https://github.com/pmpsa-cfd/aerosolved)

AeroSolved.Contact@pmi.com

The aerosol is described within an Eulerian-Eulerian framework with the aerosol size distribution and aerosol dynamics represented by either a sectional or a two-moment method. The framework is able to capture all main aerosol physics, including evaporation, nucleation, drift, Brownian diffusion, and deposition.

CFD Investigations

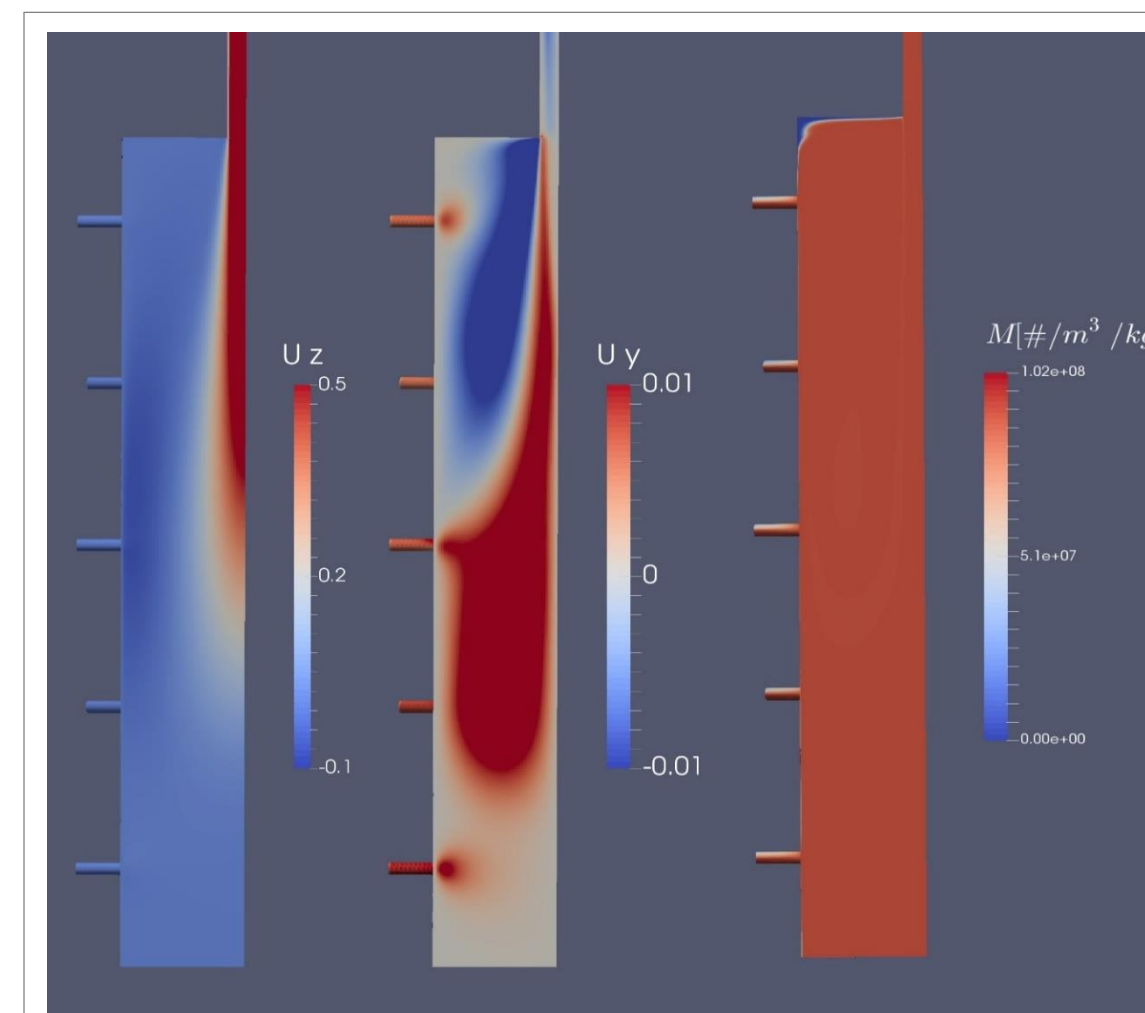


Figure 3: Vertical velocity (U_z [m/s]), horizontal velocity (U_y [m/s]), and particle number density (M) for particles of diameter 1.7 μm in a plane inside the NOEC inner chamber at steady-state conditions.

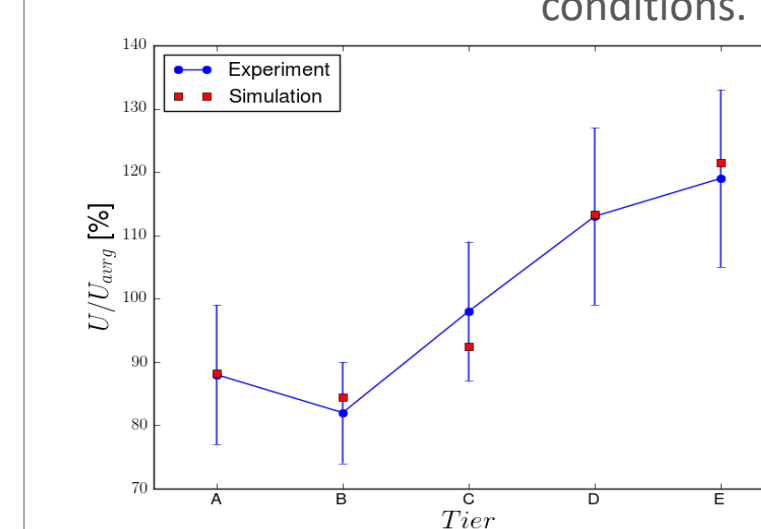


Figure 6: Port velocity at each tier expressed as percentage of the average value. CFD and experimental values are compared.

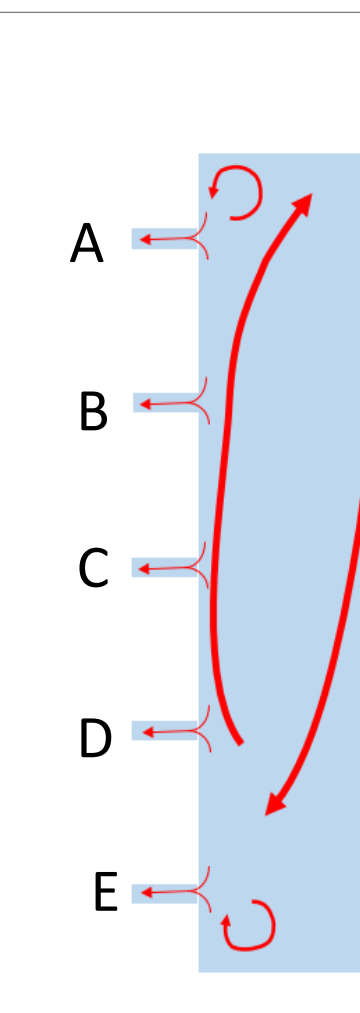


Figure 4: Schematic of the flow inside the inner chamber.

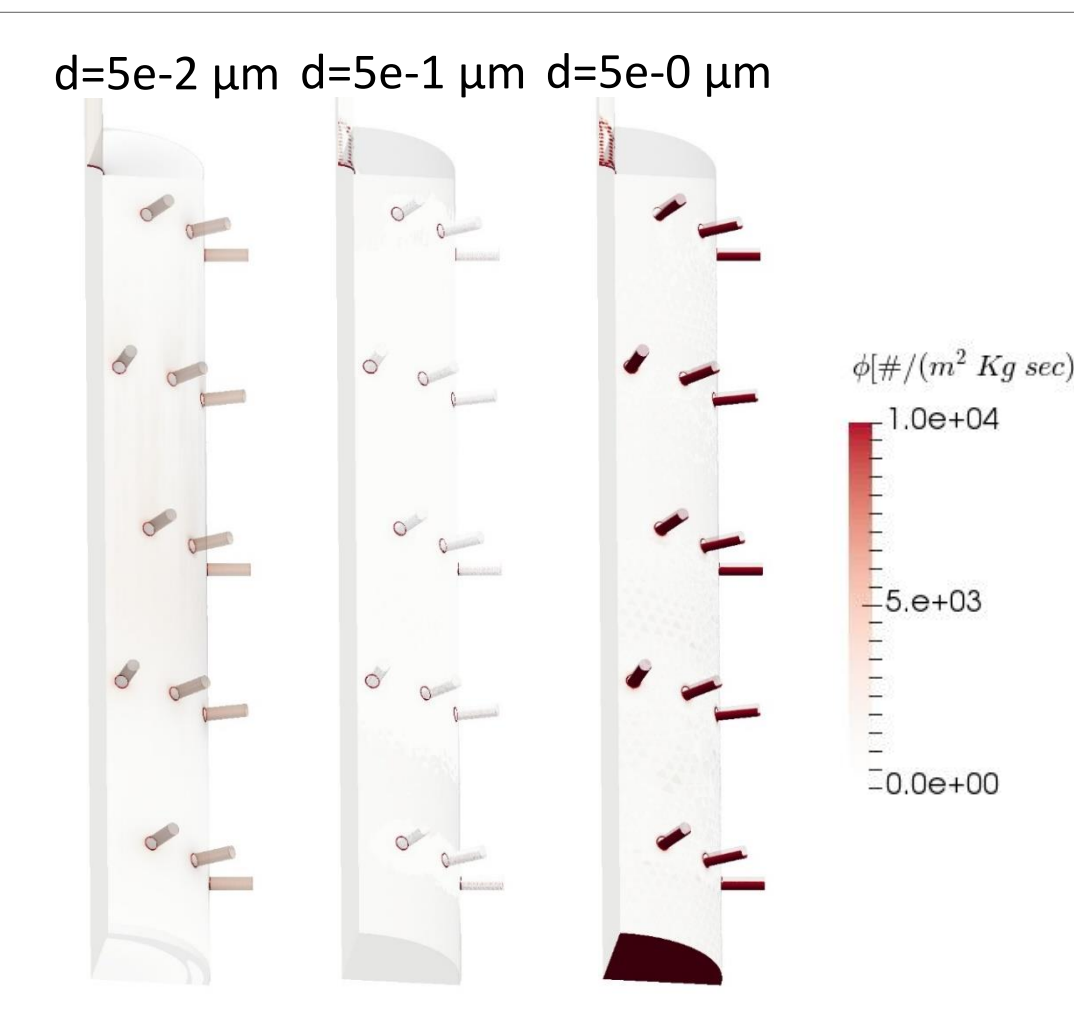


Figure 5: Deposition fluxes on the inner chamber walls for three diameters (0.05, 0.5, and 5 μm) of PSL particles.

CFD simulations were performed to investigate the NOEC system and identify possible critical factors in the system homogeneity and sampling. A 90° section of the inner chamber was modelled to analyze the complex flow structure inside the NOEC. The main central jet was observed to recirculate upward (Figures 3 & 4). As a result, a higher pressure at the bottom of the chamber was observed, causing a relatively higher flow through the port of the lower tiers (Figure 6). Deposition losses were localized mainly at the port entrance and on the horizontal wall surfaces (Figure 5).

The assembly of the exposure port and nose (Figure 7) was modelled to investigate the sampling at the mouse nostrils. To facilitate the simulations, constant breathing was assumed, and flow rates up to an equivalent peak inspiratory flow of 450 mL/min was analyzed. Although some aerosol separation was observed due to sedimentation for the larger particles (Figure 8), only a small (~1%) sampling at the mouse nose was observed (Figure 9). Currents efforts are trying to verify the present results under normal oscillatory breathing patterns.

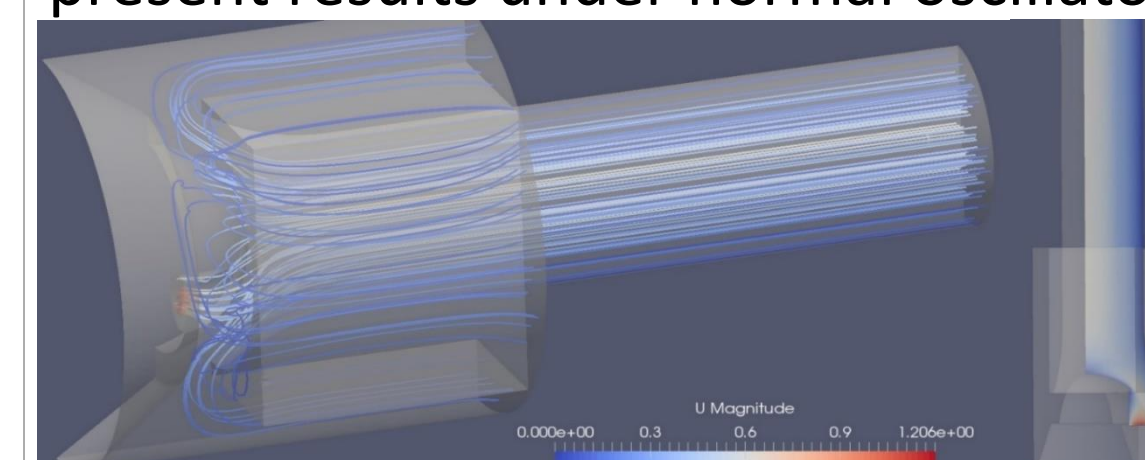


Figure 7: CFD investigation of the nose-port assembly. Flow streamlines (left) and velocity contours (right) in the case of steady 150mL/min respiratory minute volume.

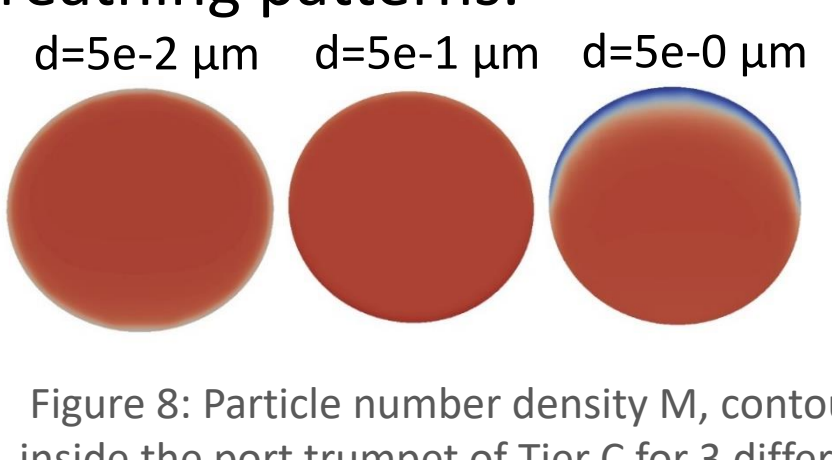


Figure 8: Particle number density M , contours inside the port trumpet of Tier C for 3 different particle diameters (i.e., 0.05, 0.5, and 5 μm). Contours are taken 2.0 cm from the port inlet from the inner chamber.

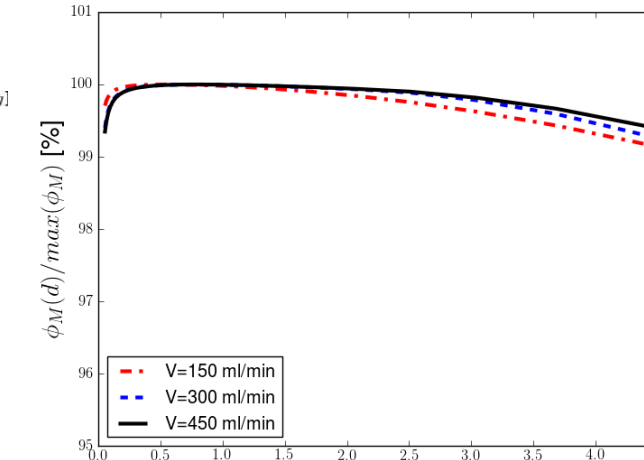


Figure 9: Sampling variability in the nose-port assembly, three different constant respiratory minute flows.

Experimental Investigations

Experimental studies were conducted to investigate the flow and aerosol homogeneity among the ports of the NOEC in the 60-port configuration. Air velocities at different ports were measured using a thermoelectric probe. With a modified inlet tube of 49 mm diameter, the velocity variation between all ports was reduced from 20% to 10% (Figure 10). A TSI Aerodynamic Particle Sizer (APS) was used to measure the PSL particle homogeneity. Particles were generated using a TSI Constant Output Generator. PSL particles of 0.6, 1.0, and 1.6 μm diameters were tested. A minimum concentration of 90% (std=11%) relative to the value at the inner chamber inlet was measured.

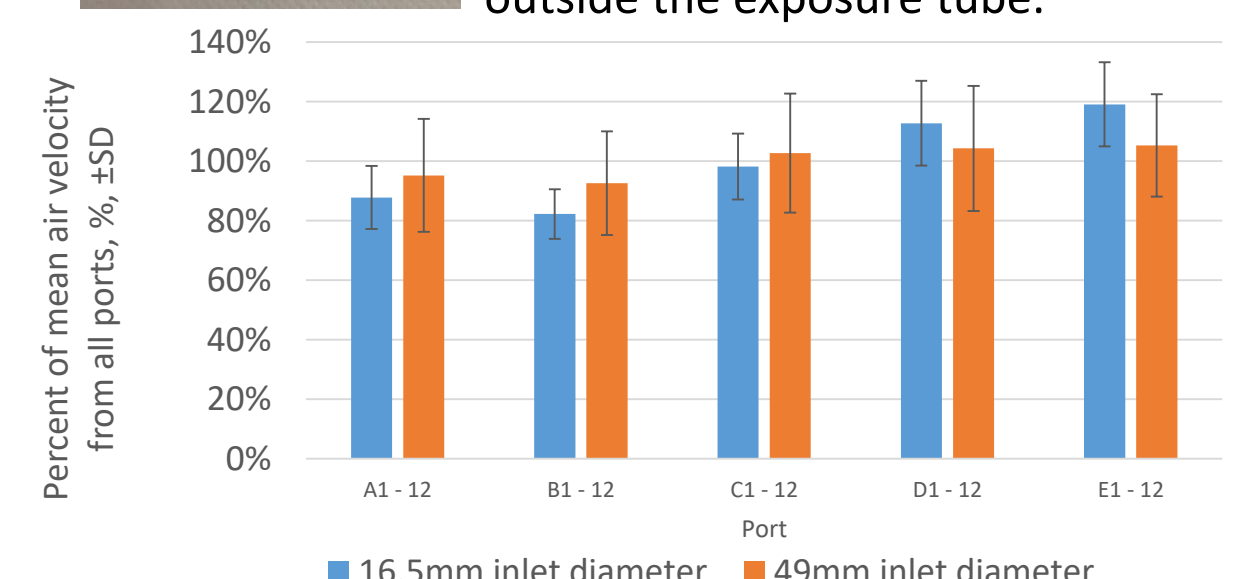
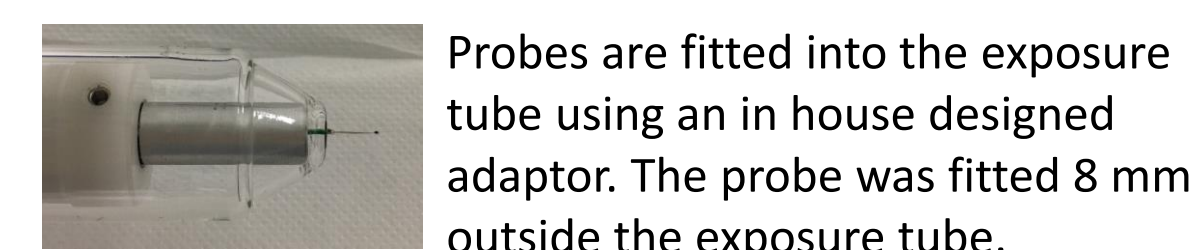


Figure 10: Mean air velocity from all ports of each tier expressed as a percentage of the mean air velocity from all ports in a 60-port NOEC probe at 8 mm outside exposure tube. Two inlet tubes were tested: the standard diameter (16.5 mm) and a modified one (49 mm).

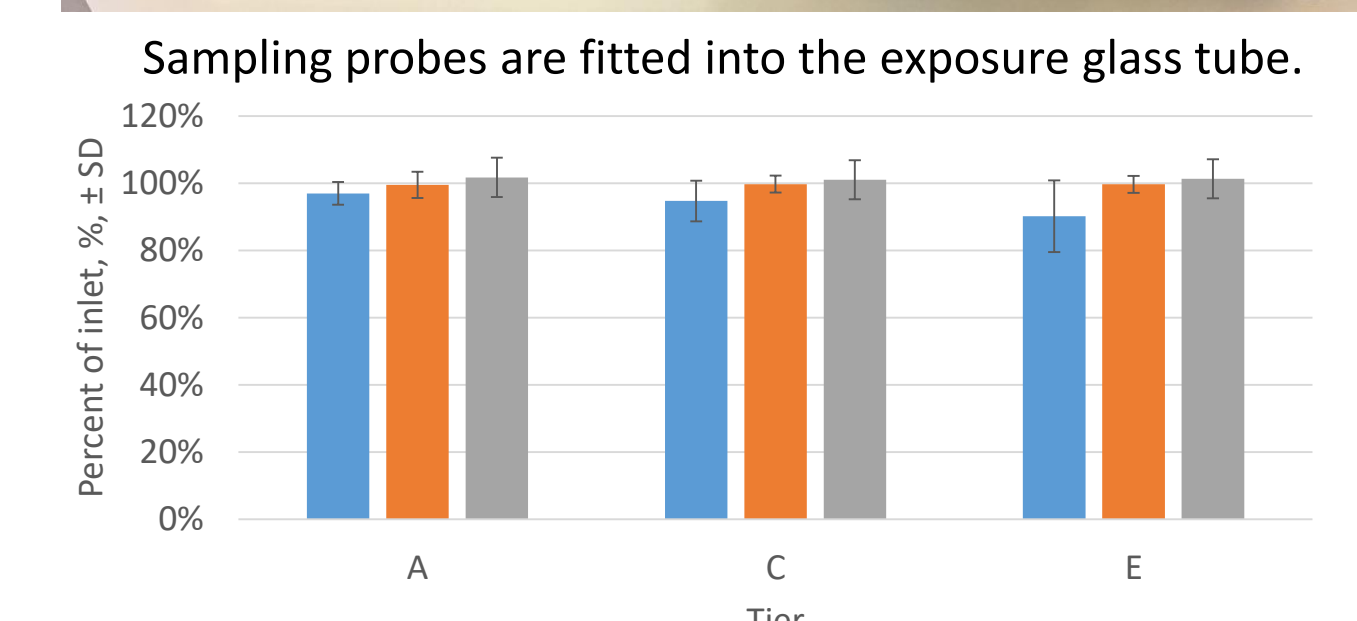


Figure 11: Particle concentration measured in glass pipe in front of the NOEC expressed as percentage relative to the NOEC inner chamber inlet (4-6 hours).

Concluding Remarks

- Flow and aerosol sampling were investigated both experimentally as well computationally with a good agreement and understanding of the exposure chamber functioning.
- Under operational conditions, a maximum flow variability of 20% was observed among all ports. This variability does not affect particles concentrations at the ports and can be reduced by increasing the diameter of the inner chamber inlet. Rotation of the experimental animals in the NOEC may further increase the homogeneity of the exposure.
- Sampling variability among ports was experimentally verified to be within 10% for particles in the range of the diameters between 0.56 < d < 1.7 μm (the maximum sampling variation was observed for the smaller particles – quantification near the lower limit of the APS).
- By assuming a constant inhalation flow, we have computationally verified a very small (< 1%) preferential aerosol sampling at the mouse nose, which will be verified by imposing a oscillating breathing pattern.

